The Influence of Printing Materials on Shrinkage Characterization in Metal 3D Printing using Material Extrusion Technology

Thi Van Nga Tran
Faculty of Mechanical Engineering, University of Transport and Communications, Vietnam
ngattv@utc.edu.vn

Dang Cao Long
Faculty of Mechanical Engineering, Vinh Long University of Technology Education, Vietnam
caodanglong.quatest3@gmail.com

Cuong Nguyen Van
Faculty of Mechanical Engineering, University of Transport and Communications, Vietnam
nguyencuong@utc.edu.vn (corresponding author)

Received: 7 May 2024 | Revised: 19 May 2024 and 29 May 2024 | Accepted: 31 May 2024

Licensed under a CC-BY 4.0 license | Copyright (c) by the authors | *DOI: https://doi.org/10.48084/etasr.7758*

ABSTRACT

This study investigates the shrinkage characteristics of various materials in metal 3D printing using Material Extrusion (ME) technology. The materials examined include 17-4PH Stainless Steel V1 and V2, Inconel 625, H13 Tool Steel V1, and A2 Tool Steel. Experiments reveal that shrinkage rates vary significantly among these materials, with 17-4PH Stainless Steel V1 exhibiting the lowest average shrinkage rate of 16.2%, while Inconel 625 shows the highest average shrinkage rate of 24.5%. These findings are critical for improving dimensional accuracy in metal 3D printing. Additionally, results demonstrate that print orientation affects shrinkage. The analysis of product accuracy reveals inconsistencies between printed dimensions and design specifications, likely influenced by printing parameters. The conclusion underscores the importance of selecting appropriate printing materials and optimizing parameters to ensure dimensional accuracy in 3D printed products.

Keywords-additive manufacturing; material extrusion; 3D printing; shrinkage; print quality; 17–4 PH stainless steel; mechanical properties

I. INTRODUCTION

Additive Manufacturing (AM) technology is revolutionizing how engineers and designers create products by enhancing design freedom [1, 2]. Nowadays, AM machines are rapidly evolving, transitioning into efficient systems for mass-producing flexible product lines. Without the need for machining or molds, AM reduces manufacturing costs to a per-unit basis. Particularly in metal product manufacturing, interest is rapidly growing because AM allows for the creation of nearly limitless intricacies with complex structures, using exceptional materials [3]. In fact, the primary advantage of AM over traditional methods lies in its ability to optimize product functionality through design freedom [4, 5].

Desktop Metal Inc. and Markforged Inc. have introduced innovative machines combining Fused Deposition Modeling (FDM) for polymers with Metal Injection Molding (MIM) [6]. Desktop Metal Inc. calls their printing process Bound Metal DepositionTM (BMD), while Markforged Inc. refers to theirs as Atomic Diffusion Additive Manufacturing (ADAM). These processes employ a filament comprising metal powder mixed with a thermoplastic polymer, serving as a binding agent for the metal particles [7]. The mixed material is stored in a cartridge atop the machine and, during printing, is fed into a unit where the thermoplastic is softened for extrusion. BMD employs an ultrasonic vibrator to provide the necessary energy for bonding the extruded material with the previously deposited layers [7], whereas the Markforged Inc. system uses a heated extruder [8]. The softened material is then accumulated and pushed through a nozzle or extruder, layer by layer, onto the build plate [9]. The resulting part, known as the "green part," undergoes a washing process to remove the binder (debinding or washing operation), followed by sintering in a furnace to densify the material (sintering operation). In the Markforged Inc. system, the binder undergoes complete thermal debinding in the washing system prior to the sintering phase [9]. In the Desktop Metal system, the binder is initially removed using a solvent before undergoing thermal treatment. This difference arises from the presence of the binder.

The widespread development of Material Extrusion (ME) technology in metal 3D printing is currently facing various limitations, with one of the main issues being the quality of printed products. There are many factors influencing the quality of printed products, including the impact of material shrinkage on the accuracy of printed products and printing parameters such as print orientation, print speed, layer thickness, etc. [10-12]. The shrinkage characteristics of metal parts when printed using ME technology are a critical issue in the metal printing process, as the printed parts must have accurate dimensions to compensate for shrinkage.

Several studies have explored the impact of materials on shrinkage in metal printing. Authors in [9] examined the influence of printing orientation on mechanical properties using 17–4 PH stainless steel material with ME technology. It was noted that the variation in the internal layer structure also influenced the shrinkage rate and affected the dimensions and warping of the product. The average accuracy for height and width across all orientations was found to be 98.89% and 97.85%, respectively, relative to the nominal dimensions. Authors in [13] observed varying degrees of anisotropic shrinkage, ranging from 17.1% to 20.9%, across the x to z axis, underscoring the influence of build orientation, print speed, and layer height. They found that specimens printed upright exhibited greater variability in shrinkage values compared to those printed on-edge or flatwise. Authors in [13] used steel 316L material, altering the build orientation resulting in mechanical and shrinkage anisotropy in ME Steel 316L components, with reported shrinkage values of up to 15% along the x-y axis and up to 17% along the z-axis. Authors in [14] investigated the impact of manufacturing parameters on the mechanical performance of ME Steel 316L by modifying layer height, nozzle temperature, and flow rate. Authors in [15] focused on examining how changes in manufacturing parameters affect the subsequent shrinkage behavior of ME Steel 316L components, varying layer heights at 0.1 and 0.4 mm, infill patterns (wall and line), print speeds at 20 and 50 mm/s, and nozzle temperatures at 170 and 240°C, while keeping infill density and print bed temperature constant.

The current paper presents a study on the influence of printing materials on shrinkage and the dimensions of products after printing and sintering in ME printing technology. The aim of this work is to characterize the ADAM process using Markforged Metal X, the only commercial system currently available on the market. To assess the impact of material shrinkage in ME printing technology, the team utilized Markforged's 3D printing software and obtained product specifications for several different material types. The available material, 17-4 PH, which Markforged claims to be suitable for industrial production, was selected for experimentation. The dimensions of the test prints using 17-4 PH material were compared and evaluated against a design reference using non-contact measurement technology.

II. MATERIALS AND METHODS

A. Shrinkage Characterization

The dimensions of both the "green" metal-polymer and sintered metal specimens were assessed using Markforged's system software. The Shrinkage Rate (SR) is computed by (1):

$$SR = \frac{s_{green} - s_{sintered}}{s_{green}} x100\% \tag{1}$$

where s_{green} represents the dimensions of the pre-debinding and sintering ("green") specimen, and $s_{sintered}$ denotes the dimensions of the final (sintered) specimen along the x, y, and z axes.

The experimental printed sample is a standard-sized tensile test specimen (Figure 1).

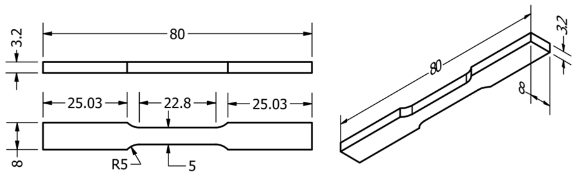

Fig. 1. The size of the printed sample.

The structure of the infill pattern depends on the printing orientation, as shown in Figure 2. The layer height is chosen as 0.127 mm. The fill pattern is triangular. The roof and floor layers are 0.51 mm post-sintered, the wall layers are 1.02 mm post-sintered (Figure 3). With the same product dimensions and printing settings as above, a survey was conducted using six different types of materials. The influence of printing materials on parameters such as Printed Dimensions, Print Time, Wash Time, Dry Time, Printed Part Mass, Final Part Mass, and Metal Volume is presented in Table I.

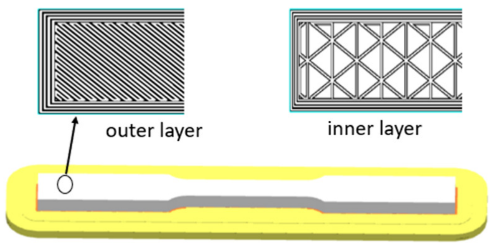

Fig. 2. The structure of the infill pattern.

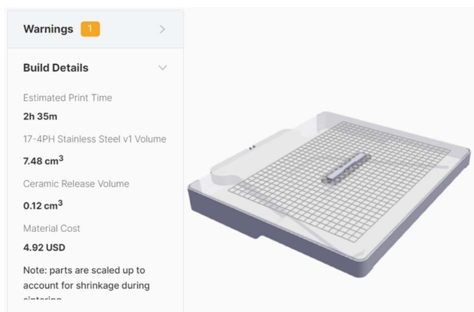

Fig. 3. Setting up the printing mode on Markforge's software.

TABLE I. INFLUENCE OF PRINTING MATERIALS ON PRINTED DIMENSIONS AND PRINTING PROCESS PARAMETERS

Material	**Printed dimensions (mm×mm ×mm)**	**Design dimensions of the part (mm×mm ×mm)**	**Print time**	**Wash time (h)**	**Dry time (h)**	**Printed part mass (g)**	**Final part mass (g)**	**Metal volume (cm^3)**
17-4PH Stainless Steel V1	95.6×9.6×3.8	80.0×8.0×3.2	1h 39m	4	1	37.8	9.41	7.48
17-4PH Stainless Steel V2	94.2×9.4×3.8	80.0×8.0×3.2	2h 49m	6	4	42.64	9.31	8.52
Inconel 625	96.3×9.6×3.8	80.0×8.0×3.2	2h 40m	4	1	41.7	10.14	7.56
H13 Tool Steel V1	95.6×9.6×3.8	80.0×8.0×3.2	2h 35m	4	1	38.03	9.49	7.48
H13 Tool Steel V1	93.2×9.3×3.7	80.0×8.0×3.2	2h 52m	12	4	45.75	NaNg	8.79
A2 Tool Steel	95.6×9.6×3.8	80.0×8.0×3.2	4h6m	4	1	38.95	9.38	7.53

B. Accuracy

Accuracy comprises two parameters: trueness and precision. Trueness in 3D printing refers to how closely the printed object matches its actual dimensions, while precision measures the consistency of repeated prints [16, 17]. High trueness indicates minimal deviation from the original object's dimensions, while high precision reflects the printer's ability to reproduce the same dimensions across multiple prints [18]. Despite existing studies on printed object accuracy, research specifically focused on the accuracy of 3D printed functional models remains limited in the literature [19].

To assess the precision of the printed product's dimensions against the design specifications, the experimental samples were printed flat. A composite of 17–4 PH stainless steel and a polymer served as the material for the material extrusion 3D printer [20]. These test samples were produced using the Markforged Metal X, as depicted in Figure 4.

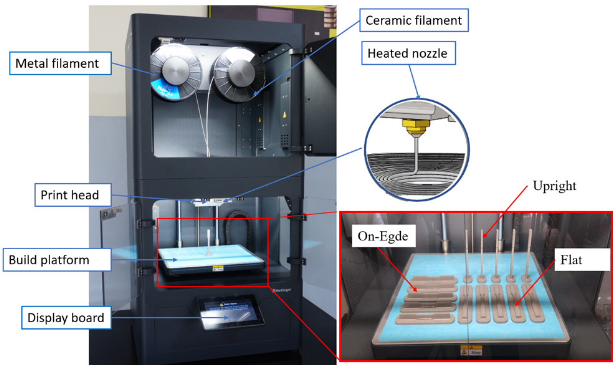

Fig. 4. Experiments on the ME machine.

To evaluate the product's accuracy relative to the design dimensions, the ATOS Compact Scan 8M system from GOM (Germany) was employed at the High-tech Center of Vinh Long University of Technical Education (Figure 5). Initially, the test sample model was designed using CAD software (Inventor, Autodesk., USA), then replicated three times using the Markforged Metal X printer. Subsequently, the printed models underwent scanning with an industrial scanner to generate corresponding digital models. These digital models were then compared to the master model, and an assessment of trueness was conducted through model superimposition. Precision was determined for each case by overlaying different combinations of the three datasets within each group.

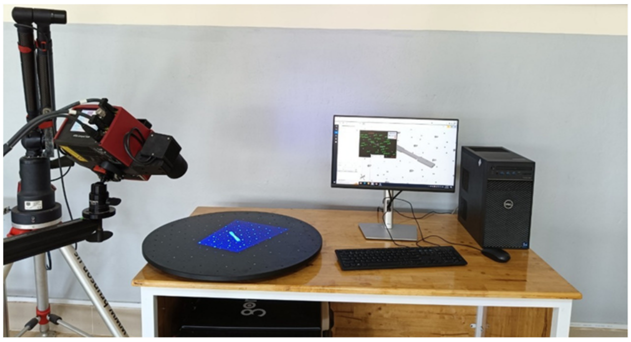

Fig. 5. Scanning the sample using ATOS Compact Scan 8M system from GOM.

III. RESULTS AND DISCUSSION

The shrinkage characteristics obtained from various materials with identical product dimensions and printing settings are summarized in Table I, namely, x (length), y (width), and z (thickness) shrinkage. The average percentage shrinkage ranged from 14.2 to 16.9% along the x-axis and from 14.0 to 16.7% along the y-axis (Figures 6-7), and 13.5 to 15.8% along the z-axis (Figure 8).

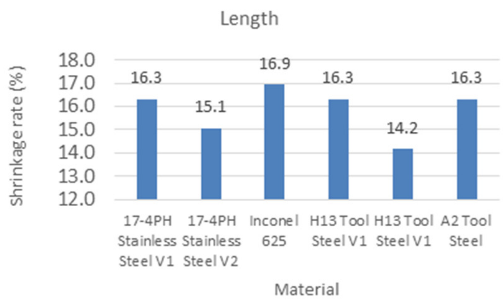

Fig. 6. Mean of x – axis (length) shrinkage.

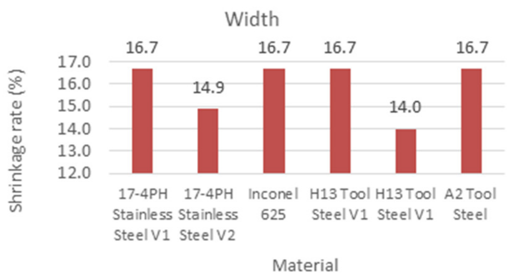

Fig. 7. Mean of y – axis (width) shrinkage.

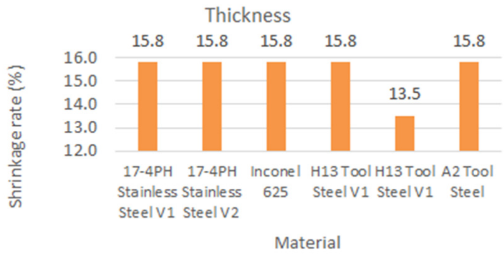

Fig. 8. Mean of z – axis (thickness) shrinkage.

Materials exhibiting high shrinkage include Inconel 625, 17-4PH stainless steel V1, and A2 Tool steel. Conversely, materials with low shrinkage include H13 Tool Steel V1 and 17-4PH stainless steel V1.

The observed variations in shrinkage among different materials can be attributed to several factors, including differences in material composition, thermal properties, and inherent characteristics specific to each material. For instance, materials like Inconel 625, 17-4PH stainless steel V1, and A2 Tool steel demonstrate high shrinkage percentages, possibly due to their unique metallurgical properties or the presence of certain alloying elements that influence the sintering process. Conversely, materials like H13 Tool Steel V1 and 17-4PH stainless steel V1 exhibit lower shrinkage percentages, indicating better dimensional stability during printing and sintering. Moreover, variations in shrinkage may also be influenced by printing parameters such as print orientation, layer height, and print speed, which can impact the cooling and solidification rates of the printed material. These factors collectively contribute to the observed differences in shrinkage characteristics among the materials tested. Based on the color-coded maps (Figure 9), slight contraction was observed on the buccal surfaces of the upper part of the test specimen, while mild expansion was noted on the lower surface, resulting in a slight convex curvature (Figure 10).

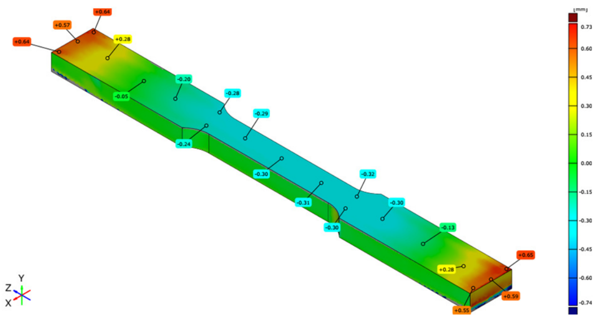

Fig. 9. Surface comparison towards CAD top side.

Additionally, circumferential shrinkage was identified. However, slight curvature and expansion were observed at both ends of the test specimen. The digital printed model underwent superimposition using the best-fit alignment method in 3D analysis software, which displayed the root mean square and average maximum and minimum values. Trueness was assessed by superimposing the data of the digital printed model onto the scanned dataset obtained from the part after printing.

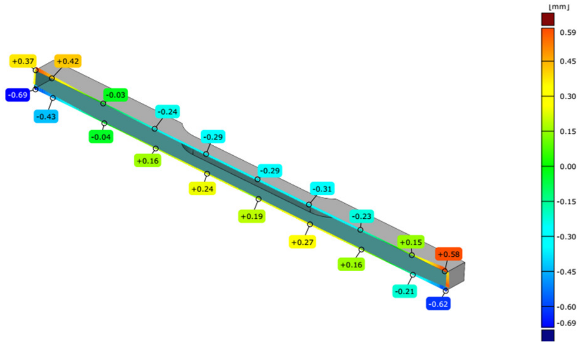

Fig. 10. Inspection section plane X.

In addition to the influence of printing materials on shrinkage affecting the dimensions of the printed product, factors such as print orientation, layer thickness, number of layers, print speed, and post-processing can affect the accuracy and precision of printed objects, leading to variations in the production of the final model.

IV. CONCLUSION

This study conducted a series of experiments to examine the impact of printing materials on the shrinkage characteristics in metal 3D printing using Material Extrusion technology. The results highlighted significant variations in shrinkage among different materials. Materials such as Inconel 625, 17-4PH stainless steel V1, and A2 Tool steel showed considerable levels of shrinkage, while H13 Tool Steel V1 and 17-4PH stainless steel V1 demonstrated lower shrinkage percentages, suggesting better dimensional stability during printing and sintering.

Moreover, the analysis of product dimensional accuracy unveiled disparities between the printed product dimensions and both the original design dimensions and the dimensions calculated by Markforged's software. These discrepancies might be ascribed to the influence of printing parameters such as print orientation, layer height, and print speed, which can impact the accuracy and stability of the printed product.

ACKNOWLEDGMENT

The work described in this paper was supported by Vinh Long University of Technology Education for a scientific project.

REFERENCES

[1] A. Vafadar, F. Guzzomi, A. Rassau, and K. Hayward, "Advances in Metal Additive Manufacturing: A Review of Common Processes, Industrial Applications, and Current Challenges," *Applied Sciences*, vol. 11, no. 3, Jan. 2021, Art. no. 1213, https://doi.org/10.3390/app11031213.

[2] D. G. Zisopol, I. Nae, A. I. Portoaca, and I. Ramadan, "A Statistical Approach of the Flexural Strength of PLA and ABS 3D Printed Parts," *Engineering, Technology & Applied Science Research*, vol. 12, no. 2, pp. 8248–8252, Apr. 2022, https://doi.org/10.48084/etasr.4739.

[3] H. Lee, C. H. J. Lim, M. J. Low, N. Tham, V. M. Murukeshan, and Y.-J. Kim, "Lasers in additive manufacturing: A review," *International Journal of Precision Engineering and Manufacturing-Green Technology*, vol. 4, no. 3, pp. 307–322, Jul. 2017, https://doi.org/10.1007/s40684-017-0037-7.

[4] I. Gibson, D. W. Rosen, B. Stucker, *Additive Manufacturing Technologies*, New York, NY, USA: Springer, 2015.

[5] Y. Saadlaoui, J.-L. Milan, J.-M. Rossi, and P. Chabrand, "Topology optimization and additive manufacturing: Comparison of conception methods using industrial codes," *Journal of Manufacturing Systems*, vol. 43, pp. 178–186, Apr. 2017, https://doi.org/10.1016/j.jmsy.2017.03.006.

[6] M. Galati and P. Minetola, "Analysis of Density, Roughness, and Accuracy of the Atomic Diffusion Additive Manufacturing (ADAM) Process for Metal Parts," *Materials*, vol. 12, no. 24, Jan. 2019, Art. no. 4122, https://doi.org/10.3390/ma12244122.

[7] T. Wohlers, "Desktop Metal targets speed, cost and high-volume production AM," *Metal Additive Manufacturing*, vol. 3, no. 2, Jun. 2017, Accessed: Jun. 04, 2024. [Online]. Available: https://www.metal-am.com/articles/desktop-metal-targets-speed-cost-and-high-volume-production-3d-printing/.

[8] "The Best Metal 3D Printing Materials for Additive Manufacturing," Markforged. https://markforged.com/resources/blog/metal-3d-printing-materials.

[9] L. C. Dang, C. V. Nguyen, A. H. Le, and D. T. Bui, "A Study on the Influence of Printing Orientation in Metal Printing Using Material Extrusion Technology on the Mechanical Properties of 17-4 Stainless Steel Products," *Journal of Machine Engineering*, vol. 23, no. 4, pp. 89–100, Dec. 2023, https://doi.org/10.36897/jme/170509.

[10] T. Kurose *et al.*, "Influence of the Layer Directions on the Properties of 316L Stainless Steel Parts Fabricated through Fused Deposition of Metals," *Materials*, vol. 13, no. 11, Jan. 2020, Art. no. 2493, https://doi.org/10.3390/ma13112493.

[11] C. Tosto, J. Tirillò, F. Sarasini, C. Sergi, and G. Cicala, "Fused Deposition Modeling Parameter Optimization for Cost-Effective Metal Part Printing," *Polymers*, vol. 14, no. 16, Jan. 2022, Art. no. 3264, https://doi.org/10.3390/polym14163264.

[12] M. Á. Caminero, A. Romero, J. M. Chacón, P. J. Núñez, E. García-Plaza, and G. P. Rodríguez, "Additive manufacturing of 316L stainless-steel structures using fused filament fabrication technology: mechanical and geometric properties," *Rapid Prototyping Journal*, vol. 27, no. 3, pp. 583–591, Jan. 2021, https://doi.org/10.1108/RPJ-06-2020-0120.

[13] T. Kurose *et al.*, "Influence of the Layer Directions on the Properties of 316L Stainless Steel Parts Fabricated through Fused Deposition of Metals," *Materials*, vol. 13, no. 11, Jan. 2020, Art. no. 2493, https://doi.org/10.3390/ma13112493.

[14] C. Tosto, J. Tirillò, F. Sarasini, C. Sergi, and G. Cicala, "Fused Deposition Modeling Parameter Optimization for Cost-Effective Metal Part Printing," *Polymers*, vol. 14, no. 16, Jan. 2022, Art. no. 3264, https://doi.org/10.3390/polym14163264.

[15] M. Quarto, M. Carminati, and G. D'Urso, "Density and shrinkage evaluation of AISI 316L parts printed via FDM process," *Materials and Manufacturing Processes*, vol. 36, no. 13, pp. 1535–1543, Oct. 2021, https://doi.org/10.1080/10426914.2021.1905830.

[16] A. Ender and A. Mehl, "Accuracy of complete-arch dental impressions: A new method of measuring trueness and precision," *The Journal of Prosthetic Dentistry*, vol. 109, no. 2, pp. 121–128, Feb. 2013, https://doi.org/10.1016/S0022-3913(13)60028-1.

[17] *ISO 5725-1:2023. Accuracy (trueness and precision) of measurement methods and results. Part 1: General principles and definitions*, 2nd ed. ISO, 2023.

[18] M. Revilla-León, M. J. Meyers, A. Zandinejad, and M. Özcan, "A review on chemical composition, mechanical properties, and manufacturing work flow of additively manufactured current polymers for interim dental restorations," *Journal of Esthetic and Restorative Dentistry*, vol. 31, no. 1, pp. 51–57, 2019, https://doi.org/10.1111/jerd.12438.

[19] M.-E. Park and S.-Y. Shin, "Three-dimensional comparative study on the accuracy and reproducibility of dental casts fabricated by 3D printers," *The Journal of Prosthetic Dentistry*, vol. 119, no. 5, pp. 861.e1-861.e7, Dec. 2018, https://doi.org/10.1016/j.prosdent.2017.08.020.

[20] C. N. Van, A. L. Hoang, C. D. Long, and D. N. Hoang, "Surface Roughness in Metal Material Extrusion 3D Printing: The Influence of Printing Orientation and the Development of a Predictive Model," *Engineering, Technology & Applied Science Research*, vol. 13, no. 5, pp. 11672–11676, Oct. 2023, https://doi.org/10.48084/etasr.6162.